

This is the accepted manuscript made available via CHORUS. The article has been published as:

Tuning the catalytic property of nitrogen-doped graphene for cathode oxygen reduction reaction

Yexin Feng, Feifei Li, Zhenpeng Hu, Xiaoguang Luo, Lixin Zhang, Xiang-Feng Zhou, Hui-Tian Wang, Jing-Jun Xu, and E. G. Wang

Phys. Rev. B **85**, 155454 — Published 26 April 2012

DOI: [10.1103/PhysRevB.85.155454](https://doi.org/10.1103/PhysRevB.85.155454)

Tuning the Catalytic Property of Nitrogen Doped Graphene for Cathode Oxygen Reduction Reaction

Yexin Feng,¹ Feifei Li,¹ Zhenpeng Hu,¹ Xiaoguang Luo², Lixin Zhang^{1*}, Xiang-Feng Zhou,¹ Hui-Tian Wang,¹
Jing-Jun Xu,¹ and E. G. Wang³

¹*School of Physics, Nankai University, Tianjin 300071, P. R. China*

²*School of Electronic Engineering, Nankai University, Tianjin 300071, P. R. China*

³*School of Physics, Peking University, Beijing 100871, P. R. China*

Abstract

Based on first principles method, the catalytic property of nitrogen-doped graphene is investigated for cathode oxygen reduction reaction. It is revealed that nitrogen clusters other than isolated one are the most efficient catalytic sites for oxygen reduction. Codoping boron (or Fe, Co) can effectively stabilize these otherwise high energy clusters while keep the cluster's high activity. Clusters with three or four nitrogens are found to be optimal. Theoretically catalytic properties similar to or even superior to platinum can be obtained. The results can act as guiding principles for designing new functional materials via codoping.

PACS numbers(s): 82.45.Jn, 88.30.-k, 81.05.U-, 68.43.Bc

* corresponding author, email: lxzhang@nankai.edu.cn

For low-temperature hydrogen fuel cell, oxygen reduction reaction (ORR) at the cathode is the rate-limiting and key reaction step, due to its much lower reactivity than that of the anode hydrogen oxidation reaction [1]. At present, the most efficient and stable cathode catalyst is Pt [2, 3], but the expensive price and rareness on earth of the noble metal drastically hinder the commercialization of Pt-containing fuel cell technology. Therefore low-Pt loading cathode catalyst and even non-Pt cathode catalyst are receiving more and more research attention currently [3-5].

N-doped carbon alloys have shown evidence of catalytic active for cathode ORR for a long time [5, 6]. Recently it is found that N-doped carbon nanotubes and N-doped graphene both possess surprisingly high such catalytic activity [7-9]. Acting as metal-free electrode, they both possess better electro catalytic activity, long-term operation stability, and tolerance to crossover effect than Pt for ORR in alkaline fuel cells, which make them prosperous candidates to replace Pt. Meantime, a few reports claim that codoping with B atoms can greatly boost the catalytic activity of the N-doped carbon alloys [10-12]. Till now the role of B atoms and the catalytic mechanism of those N-doped carbon materials are still mysterious, which hinder the further improvement and application of such materials in fuel cell technology.

Besides, heat-treated metal (Fe or Co)-N/C systems as another kind of non-Pt cathode catalyst have been under development for several decades [13-15], starting with the pioneer works by Jasinski [16] and by Yeager and co-workers [17]. Recently much progress has been made in this system [18-21]. It is claimed that the catalytic efficiency of such catalyst has approached and even exceeded the commercial Pt-C catalysts [18-20]. What a role the metal atoms play is the key to the understanding of the mechanism of the catalytic properties. Actually the transition metal-N/C system can be regarded as another kind of carbon material codoped with N and transition metals, similar to the system of N, B codoped carbon alloy. At present whether the B and the transition metals play similar roles in the N-doped materials is untouched.

For cathode ORR, the properly adsorbed O_2 is the key catalytic intermediate throughout the entire reaction process and an appropriate adsorption energy is critical for the catalytic activity [1, 22]. For all the carbon nano materials, graphene is the proto type, the building block of carbon nanotubes, multi-layer graphene, graphite, and fullerenes etc. Graphene itself shows many unique mechanical and electrical properties. So theoretically searching for the most reactive adsorption sites in N-doped graphene and studying the adsorption energy of O_2 at these sites are very important for the development of Pt replacement carbon based catalysts.

In this paper, based on first principles calculations, we find that at the substitutional N site (N_C) in graphene, the adsorption energy of O_2 is enhanced from 0.07eV on pristine graphene to 0.18eV. But the adsorption energy is still far from that on the Pt(111) surface, which is ~ 1 eV. By forming N_C clusters, the adsorption energy can be increased dramatically. For clusters comprised of three and four N_C s, the adsorption energies can be as high as 1.26 eV and 0.89 eV respectively, both comparable to

that on the Pt(111) surface. We also find that B and transition metals like Fe and Co can significantly stabilize these otherwise high energy clusters while keep the high adsorbing ability to O₂. Bader charge analyses [23] show that the more N_Cs in the cluster, the more charges transferred to the adsorbed O₂, and the higher the adsorption energies. This indicates that in order to design efficient Pt replacement catalysts in carbon materials, deliberately forming N_C clusters with at least three N_Cs in low dimensional carbon materials is the key. Codoping with B (or Fe, Co) can effectively stabilize these N_C clusters while keep their high catalytic properties.

Spin-polarized density-functional theory calculations are performed using the Vienna *ab initio* simulation package (VASP) [24]. The Kohn-Sham one-electron wave functions are expanded in a plane wave basis set with cut-off energy of 400 eV. Exchange and correlation effects are incorporated within the generalized gradient approximation (GGA) at the PW-91 level [25]. We employ a supercell of 6×6 graphene including 72 atoms as a standard model, and a slab layer of 19.2 Å thick is proved to be sufficient to render interaction energies between graphene layers. The Brillouin zone is sampled using a 3×3×1 Monkhorst-Pack grid. We consider the effect of spin polarization in all total energy calculations. The calculated equilibrium lattice constant for pristine graphene is 2.466 Å, in excellent agreement with experimental value (2.46 Å).

The formation energies of the defect complexes in graphene are given by

$$E_f = E_{\text{tot}}(m, n) - E_{\text{tot}}(0, 0) - m\mu_N - n\mu_X + (m + n')\mu_C \quad (1)$$

where m is the number of N_Cs, n is the number of X (B, Fe or Co) atoms, n' is the number of the substituted C atoms by X atoms, $E_{\text{tot}}(m, n)$ is the total energy of the supercell with the defect complex, and $E_{\text{tot}}(0, 0)$ is the total energy of the pristine graphene. The symbols μ_C , μ_X , and μ_N are the chemical potentials of C, X, and N reservoirs. For the chemical potential of N which is tunable during the experiments, we set one limit at the state of N₂, the other is in the two dimensional (2D) g-C₃N₄ phase [26, 27] with C rich condition that is defined by $4\mu_N + 3\mu_C = \Delta H(g\text{-C}_3\text{N}_4)$, where ΔH is the formation enthalpy of 2D g-C₃N₄. The μ_C is calculated as in graphene, μ_B , μ_{Fe} and μ_{Co} as in their bulk phases respectively. The adsorption energy of O₂ molecule is defined as

$$E_a = E_G + E_{\text{O}_2} - E_{\text{tot}} \quad (2)$$

where E_{tot} is the total energy of the supercell (pristine or doped graphene) with a bound O₂, E_G is the energy without O₂, and E_{O_2} is the energy of the isolated O₂ molecule.

We calculate the adsorption of O₂ on the pristine graphene sheet as the start. The atomic structure of pristine graphene is shown in Fig. 1(a). The optimal adsorption configuration of O₂ and the charge redistribution upon the adsorption (the difference between charge density of the adsorbed configuration and the sum of the charge densities of the isolated graphene and the O₂ with the adsorbed configuration respectively) are shown in the inset. The adsorption energy is 0.07 eV. This value is in the same order as that calculated on carbon nanotubes [28], fullerenes, graphene with stable

intrinsic defects, graphene nano ribbon edges for undissociated O_2 [29], which indicates that in order to obtain high adsorption energy of O_2 in nano carbon materials, the materials must be deliberately doped by alien atoms.

One N_C site in graphene is shown in Fig. 1(b). On the N-doped graphene, the O_2 molecule tends to locate at the N_C site, as shown in the inset. As expected, the adsorption energy is increased, from 0.07 eV to 0.18 eV. The problem is that the adsorption energy is still far from that on the Pt(111) surface (1.04eV, according to our calculation), as required for high efficiency ORR. Thus isolated N_C in graphene (in other low dimensional carbon materials as well) cannot act as the efficient reactive site for ORR. Bader charge analysis shows as indicated in the figure that after the substitution, N atom gets electrons (Bader charge value is negative) and the surrounding C atoms loss electrons (Bader charge value is positive). Upon adsorption O_2 gets electrons from N as shown in the inset of Fig. 1(b). Compared with the adsorption on pristine graphene as shown in Fig. 1(a), there is much more charge transferred to O_2 from the 2D sheet for the N-doped graphene. As shown in the figures the Bader charge of the adsorbed O_2 is almost doubled on the doped graphene compared with that on the pristine graphene. It is clear that the increased adsorption energy on the doped graphene is related to the charge transfer from the surrounding C atoms to the N upon the substitution. This leads us turn to N_C clusters for obtaining even higher adsorption energies. For an N_C cluster, there are more electrons transferred from graphene to the N atoms, facilitating more charge transferred to the O_2 molecule upon adsorption. Possibly we could get scalable increased adsorption energies as wanted by clustering of N_C s.

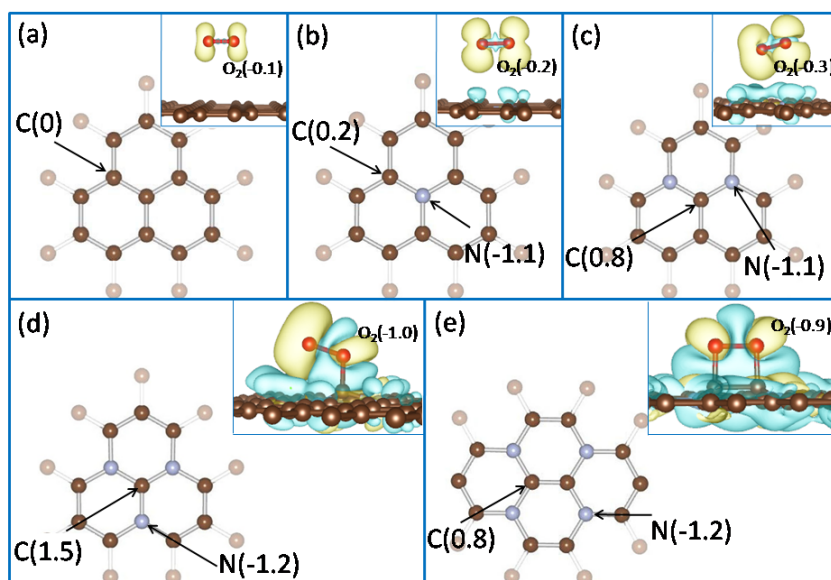


Fig. 1 (color online). The atomic structures of (a) pristine graphene, (b) one N_C , (c) two N_C , (d) three N_C , and (e) four N_C clusters in graphene. The brown balls are C atoms and the gray balls are N atoms. The Bader charge values on interested atoms are indicated in the brackets. The insets are the configurations of the adsorbed O_2 and the isosurface contours of differential charge density upon the adsorption (yellow is density gain and cyan is density loss) respectively.

The red balls are O atoms. The calculated Bader charge values on the adsorbed O₂ are indicated as well in the insets. All the contours are plotted with the charge density value of $\pm 0.001e/\text{\AA}^3$.

It is easy to understand that N_C dimers or trimers in grapheme have extreme high formation energies. Thus we just consider clusters with two, three, and four N_Cs with the configurations shown in Figs. 1(c)-1(e), in which the N_C atoms are next nearest neighbors. Calculations show that for the two N_C cluster (denoted as 2N_C), the largest adsorption energy of O₂ is 0.21 eV. The value is larger than that for one N_C but in the same order. For the cluster with three N_Cs (3N_C), the adsorption energy is significantly increased to 1.26 eV, and for the cluster with four N_Cs (4N_C), the adsorption energy is 0.89 eV, both values are comparable with that on the Pt(111) surface. The maximum adsorption energy is obtained for the 3N_C cluster. Further increasing of the size of the cluster no longer increases the adsorption energies of O₂ due to the increased area of the cluster beyond the interaction scope of O₂. The adsorption energies of the N_C clusters are plotted in Fig. 2(a). From the figure we can clearly see two regimes for the adsorption of O₂. In one regime, the adsorption energies are close to that on the Pt(111) surface, corresponding to the clusters with three and more N_Cs. In the other regime, the adsorption energies are much lower, comparable with that on pristine graphene, corresponding to the 2N_C cluster and the isolated N_C.

Back to Figs. 1(b)-1(e) in which the charge redistributions upon the adsorption of O₂ are shown in the insets, we can also see that with the number of N_Cs increased in the clusters, the charge transferred from graphene to O₂ is also increased, and the bond length of O₂ is increased accordingly, from 1.25 Å on pristine graphene to 1.49 Å on the four N_C cluster graphene. Considering all the possible configurations for the N_C clusters, we can believe that the interaction of O₂ with the N-doped graphene can be tuned, with adsorption energies from ~0 eV to ~1 eV, similar reactive properties to the Pt(111) surface can be obtained for defect clusters with 3 or more N_Cs in the graphene. The reason is that N is more electrophilic than C thus N_C can accumulate electrons from the surrounding C atoms in graphene. Oxygen is more electrophilic than N, thus O₂ can easily grab these accumulated electrons on N_Cs. In other words, with the help of N_Cs, O₂ can get more electrons from the C atoms in grapheme and the adsorption interaction on graphene thus can be monotonically increased.

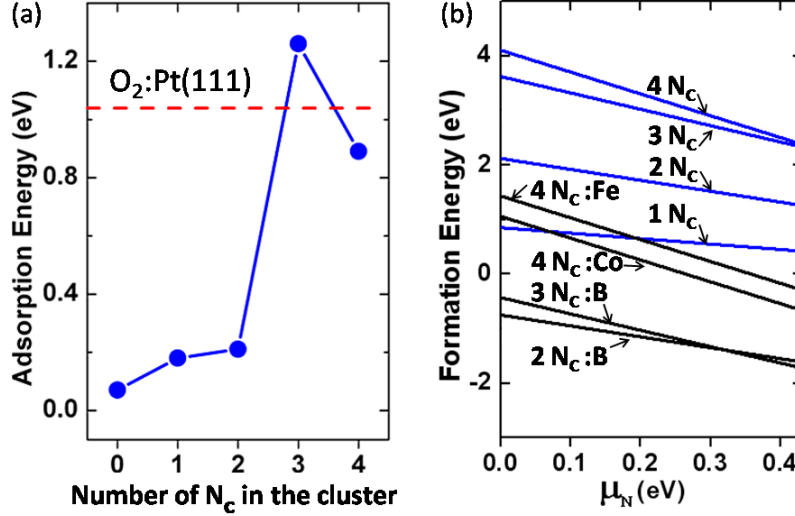


Fig. 2 (color online). (a) The adsorption energies of O_2 at clusters with different N_C numbers. The adsorption energy of O_2 on Pt(111) surface is also shown by the dashed line for comparison. (b) The formation energies of the N_C clusters and the B, Fe, and Co containing clusters (the corresponding structures are shown in Fig. 3 and Fig. 4 respectively).

But one fundamental problem is the high formation energies of these N_C clusters as shown in Fig. 2(b). At the chemical potential of N_2 , for one N_C , the formation energy is 0.85 eV. But for the four N_C cluster with the configuration shown in Fig. 1(e), the formation energy is as high as 4.2 eV. The N_C s on the graphene repel each other, so the formation energies of the N_C clusters get higher and higher, with the increasing number of N_C s in the cluster. This indicates that the larger the number of N_C s in the cluster, the lower the density of such defect clusters formed experimentally in graphene. This result is agreeable with a few reports which show that the catalytic activity of solely N-doped graphene is often very low [4, 9, 10].

B is another popular dopant in carbon materials. To our knowledge there is no report showing that solely B-doped graphene could show catalytic activity for ORR, but experiments show strong evidence that codoping carbon-based materials with N and B could enhance significantly the cathode ORR catalytic activity comparing with the solely N-doped sample [12, 13]. In order to reveal the behind mechanism and the role of B, we investigate the formation energies of B containing N_C clusters and the bonding of O_2 molecules on graphene at these cluster sites.

Boron is electronegative than C, and C is electronegative than N. Thus the B atoms tend to substitute those C atoms with the highest Bader charge values around the N_C s which can be seen from Fig. 1. We consider B containing N_C clusters with atomic structures as shown in Figs. 3(a)-3(e). The data of these defect structures are summarized in Table 1. With the chemical potential of N in N_2 , the formation energies of these structures are all lower than 0, indicating that these B containing clusters are energetically favored. As already shown in Fig. 2(b), with the increasing of the chemical potential of N, the formation energies of such clusters can be further lowered. Noting that the formation energy of single substitutional B is comparable to single N_C , the results indicate the formation energies of B

containing N_C clusters can be significantly decreased and such complex defects are much easily to form in graphene compared to any single doping. The formation energies are not sensitive to the B:N ratio of the clusters either. So we can conclude that B can effectively stabilize the unstable N_C clusters and make the N_C clusters form more easily in experiments.

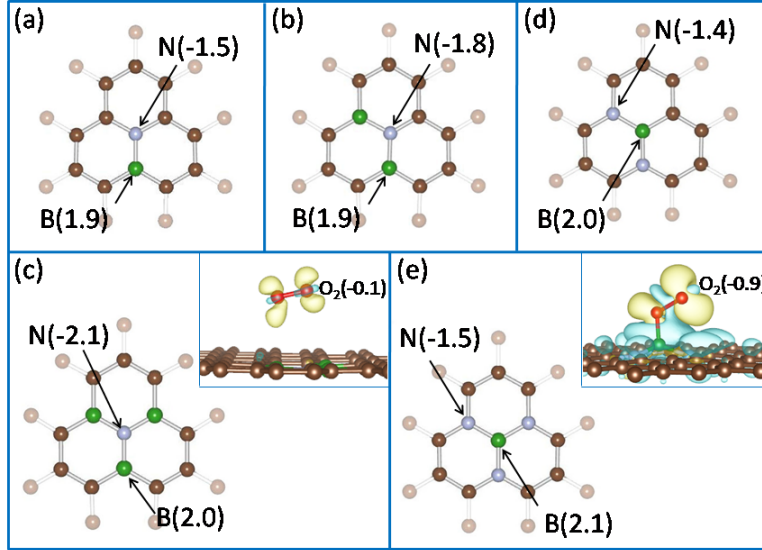


Fig. 3 (color online). The atomic structures of the B containing complexes composed of (a) one N_C and one B_C , (b) one N_C and two B_C s, (c) one N_C and three B_C s, (d) two N_C s and one B_C , and (e) three N_C s and one B_C . The calculated Bader charge values are indicated. The green balls are the B atoms. The corresponding configurations of the adsorbed O_2 molecule and the isosurface contours of differential charge density upon the adsorption (yellow is density gain and cyan is density loss) are shown in the insets in (c) and (e). The red balls are O atoms. The calculated Bader charges on the adsorbed O_2 are indicated in the insets.

TABLE 1 Structural data and the calculated results of B containing N_C clusters shown in Fig. 3. The formation energies are calculated with the chemical potential of N in N_2 .

Figures	Number of N_C	Number of B_C	Formation Energy (eV)	Bader Charges on O_2	Adsorption Energy of O_2 (eV)
(a)	1	1	-0.47	-0.12	0.07
(b)	1	2	-0.84	-0.10	0.05
(c)	1	3	-0.71	-0.12	0.05
(d)	2	1	-0.75	-0.78	0.42
(e)	3	1	-0.43	-0.86	1.30

Besides the stabilization effect of B codoping, another important issue is whether B will affect the O_2 adsorption of the N_C clusters. The calculations (summarized in Table 1) show that the O_2 adsorption energy mainly depends on how many N_C s are there in the cluster, and has almost no relation with the number of B atoms in the cluster. For example the O_2 adsorption energy at the $3N_C:B$ cluster as shown in Fig. 3(e) is 1.30eV, slightly larger than the $3N_C$ cluster without B. But for the clusters with only one N_C [shown in Figs. 3(a)-3(c)], the adsorption energies are 0.05~0.07 eV, all

comparable with one single N_C . This indicates that the B in the N_C cluster fairly affects the adsorption ability of the cluster but to stabilize the cluster and keep the adsorption ability of the N_C cluster to O_2 . This conclusion is also assisted by the Bader charge analysis of these systems. As shown in Table 1, the Bader charges on the adsorbed O_2 depends mainly on the number of N_C s in the cluster.

As far as we know from the literature, the reported high catalytic samples of N, B codoped carbon alloy all contain more N atoms than B atoms [12, 13]. Our calculations are agreeable with this fact.

Our results for the N, B codoping in graphene lead us to think that the transition metals in Fe-N/C and Co-N/C systems may act as the same role as B. That is, in Fe-N/C and Co-N/C systems, it is the N_C clustering dominates the catalytic properties. The transition metals not only can stabilize the N_C cluster, but also can keep the catalytic property of the N_C clusters.

We just confine our studies on the $3N_C$ and $4N_C$ clusters as the structures shown in Fig. 1 due to the low reactivity of the $2N_C$ cluster. Similar to the case of B containing clusters, if we just replace one C with the transition metals, we have the optimized structures as shown in Figs. 4(a) and 4(b) for $3N_C$ clusters. Unlike B, Fe or Co has larger atomic radii. From the optimized structures (metal atoms no longer in the same plane as the C atoms) it is clear that the formation energies should be very high. So most likely Fe or Co will form clusters with N_C s as shown in Figs. 4(c) and 4(d), in which the transition metals substitute two carbon atoms and surrounded by four N_C s, similar to the reported case of the N-doped carbon nanotube [20]. The formation energies of such transition metal containing clusters are already shown in Fig. 2(b). We can see that although the formation energies are higher than that of the B containing clusters, they are much lower than that of the pure N_C clusters. With the higher chemical potential of N, the formation energies can be less than 0 as well. This means that the forming of such clusters can be energetically favored by tuning the chemical potential of N.

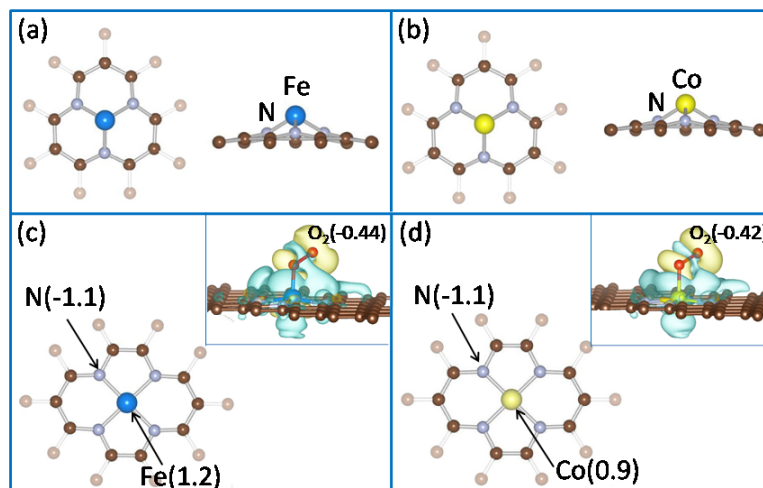


Fig. 4 (color online). The atomic structures of the complexes composed of (a) three N_C s and one Fe, (b) three N_C s and one Co, (c) four N_C s and one Fe, and (d) four N_C s and one Co. In (a) and (b) both the top and side views of the structures are shown. In (c) and (d) the calculated Bader charges on the interested atoms are indicated. The

corresponding configurations of the adsorbed O₂ molecules and the isosurface contours of differential charge density upon the adsorption (yellow is density gain and cyan is density loss) are shown in the insets of (c) and (d). The red balls are O atoms. The calculated Bader charges on the adsorbed O₂ are indicated in the insets.

The most favorable adsorption sites of O₂ on the Fe, Co containing clusters are shown in the insets of Figs. 4(c) and 4(d) and the adsorption energies are 1.11eV and 0.85eV respectively. In the two cases the O-O distance are both opened up to ~ 1.3 Å, similar to the case of the pure 4N_C cluster. This indicates that the role of the transition metal atoms in the cluster is similar to that of B, just to stabilize the cluster while keep the catalytic activity of the N_C cluster.

In conclusion, we have investigated the catalytic mechanism of N_C defects in graphene for cathode ORR. The N atoms attract electrons from the nearby C atoms facilitating more charge transferring from the graphene sheet to the adsorbed O₂. Thus N_C clusters are more favorable than single N_C in adsorbing O₂ and the strength relies on the number of N_Cs in the cluster and is tunable. But the high formation energies of such N_C clusters are a serious issue. According to our calculations, codoping with other atoms like B, Fe or Co can stabilize these N_C clusters efficiently while keep the high catalytic activity. The results are agreeable with the experiments. The revealed mechanism can act as the guiding principles to design Pt replacement catalyst in carbon nano materials.

The work is supported by the National Science Foundation of China with grant No. 11074128, National 973 Program of China with No. 2011CB922102, and by the Fundamental Research Funds for the Central Universities with No. 65030091.

References

- [1] J. K. Nørskov, J. Rossmeisl, A. Logadottir, L. Lindqvist, J. R. Kitchin, T. Bligaard, and H. Jónsson, *J. Phys. Chem. B* **108**, 17886 (2004).
- [2] S. Litster, G. McLean, *J. Power Sources* **130**, 61 (2004).
- [3] J. H. Wee, K. Y. Lee, and S. H. Kim, *J. Power Sources* **165**, 667 (2007).
- [4] Y. Bing, H. Liu, L. Zhang, D. Ghosh, and J. Zhang, *Chem. Soc. Rev.* **39**, 2184 (2010).
- [5] Y. Shao, J. Sui, G. Yin, and Y. Gao, *Appl. Catal. B* **79**, 89 (2008).
- [6] J. Ozaki, S. Tanifuji, N. Kimura, A. Furuichi, and A. Oya, *Carbon* **44**, 1324 (2006).
- [7] K. Gong, F. Du, Z. Xia, M. Durstock, and L. Dai, *Science* **323**, 760 (2009).
- [8] L. Qu, Y. Liu, J. B. Baek, and L. Dai, *ACS Nano*. **4**, 1321 (2010).
- [9] Y. Shao, S. Zhang, M. H. Engelhard, G. Li, G. Shao, Y. Wang, J. Liu, I. A. Aksay, and Y. Lin, *J. Mater. Chem.* **20**, 7491 (2010).
- [10] S. F. Huang, K. Terakura, T. Ozaki, T. Ikeda, M. Boero, M. Oshima, J. Ozaki, and S. Miyata, *Phys. Rev. B* **80**, 235410 (2009).
- [11] J. Ozaki, N. Kimura, T. Anahara, and A. Oya, *Carbon* **45**, 1847 (2007).
- [12] J. Ozaki, T. Anahara, N. Kimura, and A. Oya, *Carbon* **44**, 3358 (2006).
- [13] C. W. B. Bezerra, L. Zhang, K. Lee, H. Liu, A. L. B. Marques, E. P. Marques, H. Wang, and J. Zhang, *Electrochim. Acta* **53**, 4937 (2008).
- [14] U. I. Koslowski, I. Abs-Wurmbach, S. Fiechter, and P. Bogdanoff, *J. Phys. Chem. C* **112**, 15356 (2008).
- [15] P. H. Matter, E. Wang, J.-M. M. Millet, and U. S. Ozkan, *J. Phys. Chem. C* **111**, 1444 (2007).
- [16] R. Jasinski, *Nature* **201**, 1212 (1964).
- [17] S. Gupta, D. Tryk, I. Bae, W. Aldred, and E. Yeager, *J. Appl. Electrochem.* **19**, 19 (1989).
- [18] M. Lefèvre, E. Proietti, F. Jaouen, and J.-P. Dodelet, *Science* **324**, 71 (2009).
- [19] G. Wu, K. L. More, C. M. Johnston, and P. Zelenay, *Science* **332**, 443 (2011).
- [20] D. H. Lee, W. J. Lee, W. J. Lee, S. O. Kim, and Y.-H. Kim, *Phys. Rev. Lett.* **106**, 175502 (2011).
- [21] W. Orellana, *Phys. Rev. B* **84**, 155405 (2011).
- [22] L. Qi, X. Qian, and J. Li, *Phys. Rev. Lett.* **101**, 146101, (2008)
- [23] W. Tang, E. Sanville, and G. Henkelman, *J. Phys. Condens. Matter* **21**, 084204 (2009); E.

- Sanville, S. D. Kenny, R. Smith, and G. Henkelman, *J. Comp. Chem.* **28**, 899 (2007); G. Henkelman, A. Arnaldsson, and H. Jónsson, *Comput. Mater. Sci.* **36**, 254 (2006).
- [24] G. Kresse and J. Hafner, *Phys. Rev. B* **47**, R558 (1993); *Phys. Rev. B* **49**, 14251 (1994).
- [25] J. P. Perdew, J. A. Chevary, S. H. Vosko, K. A. Jackson, M. R. Pederson, D. J. Singh, and C. Fiolhais, *Phys. Rev. B* **46**, 6671 (1992).
- [26] L. Yang, P. W. May, L. Yin, R. Brown, and T. B. Scott, *Chem. Mater.* **18**, 5058 (2006).
- [27] A. Thomas, A. Fischer, F. Goettmann, M. Antonietti, J.-O. Müller, R. Schlögl, and J. M. Carlsson, *J. Mater. Chem.* **18**, 4893 (2008).
- [28] P. Giannozzi, R. Car, and G. Scoles, *J. Chem. Phys.* **118**, 1003 (2003).
- [29] Y. Feng and L. Zhang, unpublished.